www.elsevier.com/locate/ijadhadh

Comparison of fracture behavior between acrylic and epoxy adhesives

Makoto Imanaka, Xinwei Liu, Masaki Kimoto

PII: S0143-7496(17)30029-5
DOI: http://dx.doi.org/10.1016/j.ijadhadh.2017.02.011
Reference: JAAD1970

To appear in: *International Journal of Adhesion and Adhesives*

Received date: 18 July 2016
Accepted date: 21 January 2017

Cite this article as: Makoto Imanaka, Xinwei Liu and Masaki Kimotc Comparison of fracture behavior between acrylic and epoxy adhesives *International Journal of Adhesion and Adhesives* http://dx.doi.org/10.1016/j.ijadhadh.2017.02.011

Comparison of fracture behavior between acrylic and epoxy adhesives

Makoto Imanaka[a*], Xinwei Liu[a], Masaki Kimoto[b]

[a]Department of Technology Education, Osaka University of Education, Asahigaoka, Kashiwara, Osaka, 582-8582, Japan

[b]Department of Chemistry and Environment, Technology Research Institute of Osaka Prefecture, Izumi, Osaka 594-1157, Japan

[*]Corresponding author. E-mail address: imanaka@cc.osaka-kyoiku.ac.jp

Abstract

An experimental study was conducted on the strength of adhesively bonded steel joints, prepared epoxy and acrylic adhesives. At first, to obtain strength characteristics of these adhesives under uniform stress distributions in the adhesive layer, tensile tests for butt, scarf and torsional test for butt joints with thin-wall tube were conducted. Based on the above strength data, the fracture envelope in the normal stress-shear stress plane for the acrylic adhesive was compared with that for the epoxy adhesive. Furthermore, for the epoxy and acrylic adhesives, the effect of stress triaxiality parameter on the failure stress was also investigated. From those comparison, it was found that the effect of stress tri-axiality in the adhesive layer on the joint strength with the epoxy adhesive differed from that with the acrylic adhesive. Fracture toughness tests were then conducted under mode l loading using double cantilever beam (DCB) specimens with the epoxy and acrylic adhesives. The results of the fracture toughness tests revealed continuous crack propagation for the acrylic adhesive, whereas stick-slip type propagation for the epoxy one. Finally, lap shear tests were conducted using lap

joints bonded by the epoxy and acrylic adhesives with several lap lengths. The results of the lap shear tests indicated that the shear strength with the epoxy adhesive rapidly decreases with increasing lap length, whereas the shear strength with the acrylic adhesive decreases gently with increasing the lap length.

Keywords: Acrylic adhesive; Epoxy adhesive; Tensile strength; Torsional shear strength; Lap shear strength; Fracture toughness

1. Introduction

Adhesive bonding with carbon-fiber-reinforced plastic (CFRP) and a metallic substrate is widely used to reduce the weight of structures, and structural epoxy adhesives have been normally used for bonding these substrates. Most structural epoxy adhesives require heat curing. Hence, residual stress in the adhesive layer appears during the heart curing cycle due to the mismatch of coefficient of thermal expansion between the CFRP and metallic substrate. When joining these substrates, adhesives that can omit the heat curing process have been desired. Recently, structural acrylic adhesives have attracted special interest because the acrylic adhesive can be cured at room temperature. Another advantage is that this adhesive is available for bonding oily steel surfaces [1]. To apply these acrylic adhesives for structural bonding, it is necessary to clarify the strength characteristics of adhesively bonded joints that employ the acrylic adhesives. Hence, experimental studies on the strength of adhesively bonded joints with acrylic adhesives have been increasing: the static strength of butt and lap joints [2-7], fracture toughness [8], and durability [9] and so on. To further expand the applications of acrylic adhesives for structural bonding, it is necessary to clarify these strength

characteristics in comparison with those of the epoxy adhesives that are most widely used for structural bonding.

In this study, to compare the failure behavior between acrylic and epoxy adhesives, we selected two representative adhesives for structural use. One was a two-part toughened acrylic adhesive, and the other was a one-part epoxy adhesive that is mainly used in the automobile industry. The following items were investigated using adhesively bonded steel joints:

1) To investigate the failure criteria under combined stress conditions, the following tests were conducted: tensile tests for butt joint; torsional tests for butt joint with thin-wall tube; tensile tests for scarf joint. These joints provide considerably uniform tensile, shear and combined stress distributions in the adhesive layer, respectively [10]. Based on these data, failure envelopes for the acrylic and epoxy adhesives were compared in the normal stress- shear stress planes. Then the effect of stress triaxiality on the fracture stress for the both adhesives was also compared.

2) To compare fracture toughness between the acrylic and the epoxy adhesives, the mode I critical strain energy release rate, G_{Ic} was measured using adhesively bonded double cantilever beam (DCB) specimens.

3) Tensile shear strength of lap joints with the acrylic adhesive was compared with that of the epoxy adhesive, because the lap joint is the most popular joint type for bonding steel plates and so on. Tensile shear strengths for the acrylic and epoxy adhesives were compared with various lap lengths, and crack growth behavior for both adhesives was also investigated using crack gauges.

2. Experimental procedure

Figure 1 shows the shapes and sizes of the various adhesive-bonded specimens. The adherend used for the butt joints, scarf joints, butt joints with thin-wall tube and DCB joints was structural carbon steel (JIS S55C). Cold-reduced carbon steel (JIS SS400) was used as the adherend for lap joints. Two kinds of adhesives were used; an acrylic adhesive (C-355-20, Denka Co. Ltd.) whose curing condition is 25 h at room temperature, and a one-part epoxy adhesive (E56S, Sunrise MSI Co. Ltd.) whose curing condition is 1 hr at 435 K.

The surface preparation of the adherends was as follows. The bonding surfaces of the adherends were polished with grade 150 emery paper under dry conditions, and degreased with acetone.

Tensile tests for the butt, scarf, lap and DCB joints were conducted in an Instron-type testing machine (Shimadzu AG) at 1 mm/min cross-head speed. As shown in Fig.2(a), the relative displacement in the axial direction across the adhesive layer was measured using a clip gauge for the butt and scarf joints. Thus measured relative displacement is indicated, Δ in Figs. 5 and 6. For the DCB joints, the displacement between upper and lower loading pins was also measured using a clip gauge as in Fig.2 (b). Crack extension of the DCB joints was measured with the following procedure: a crack tip was immersed in a solution of fluorescent agent during the loading test. After unloading the specimen was broken at a cross-head speed of 500mm/min, the crack extension being measured form the fracture surface using a measuring microscope under UV light. The details was written by elsewhere [11]. For the lap joints, the machine cross-head displacement was taken as the displacement of the lap joints. Usually, cracks initiate at the two lap ends, and grow in the adhesive layer to the opposite end of the lap joint. To measure the crack growth crack form the lap end, crack

gauges (Tokyo Sokki Kenkyujo Co. Ltd.:FAC-5) were used, where the crack gauge is designed to measure the growth of the crack. In the crack gauge, the grids which are aligned with a same interval is disconnected one by one by the progress of the crack; crack growth length can be measured by the variation of the gauge resistance due to disconnection of the grids. In this experiment, the crack gages were adhered to the lap ends across the adhesive layer as in Fig.3.

Torsional tests for the butt joint with thin-wall tube were conducted in a handmade torsional testing machine at 0.015 rad/sec torsional speed. As shown in Fig.2(c), the relative rotation angle, $\Delta\theta$ across the adhesive layer was calculated based on the tangential displacement, Δd detected by a clip gauge attached to the two plates that were bonded on the radial direction of the butt joint with thin-wall tube across the adhesive layer. The relative rotation angle, $\Delta\theta$ was given by equation (1).

$$\Delta\theta = \frac{\Delta d}{r} . \qquad (1)$$

In addition, tensile tests for the bulk epoxy and acrylic adhesives were conducted using dumbbell type (JIS 7208) specimens whose shape and sizes was shown in Fig.4.

3. Experimental results and discussion

3.1 Tensile strengths of the bulk adhesive specimens, butt and scarf joints and torsional strengths of the butt joints with thin-wall tube

Figure 4 shows stress-strain curves of bulk adhesives under tensile load. As shown in this figure, brittle fracture occurred for the epoxy adhesive, whereas the acrylic adhesive exhibits clear yield behavior. Strain at the breaking point for the acrylic adhesive is over ten times higher than that for the epoxy adhesive, while the breaking strength for the epoxy adhesive is about 4 times as high as that for the

acrylic adhesive.

Figures 5 and 6 show stress-displacement curves for the butt and scarf joints bonded by the epoxy and acrylic adhesives under tensile loading, where the ordinate and the abscissa represent axial stress and relative displacement across the adhesive layer, Δ, respectively, where the ordinate, Δ was already explained in the experimental section. Similar to the stress-strain curves of the bulk adhesives, the maximum stress of the epoxy adhesive is over 4 times greater than that for the acrylic adhesive for both the butt and scarf joints. Stress tri-axiality for the dumbbell specimen is lower than that in the adhesive layer for the butt and scarf joints. Therefore, it is assumed that the yield behavior for the dumbbell specimen is more remarkable than that for the butt and scarf joints. However, brittle fracture occurred only for the dumbbell specimen with the epoxy adhesive, whereas ductile fracture occurred for the butt and scarf joint with epoxy adhesive. On the other hand, the volume of the adhesive layer for the butt and scarf joints is extremely smaller than the dumbbell specimen. Hence, the number of flaw of the dumbbell specimen is exceedingly greater than of the adhesively bonded joints. This may be one reason why the brittle fracture occurs in the dumbbell specimen, even though the stress tri-axiality for the dumbbell specimen is lower than that that of the butt and scarf joints. Figures 5 and 6 also indicate that the difference of the breaking displacement between the acrylic and the epoxy adhesives for the butt and scarf joints is smaller than the relative difference of the breaking strain between the acrylic and the epoxy adhesives for the dumbbell specimens as in Fig. 4.

Figure 7 also shows the stress-rotation angle for the butt joint with thin-wall tube under torsional loading. Similar to the butt and scarf joints, the maximum stress

of the epoxy adhesive is over 4 times than that of the acrylic adhesive. When comparing the rotation angle for fracture between the epoxy and the acrylic adhesives, the difference of rotation angle for fracture is greater than the differences of displacement for fracture of the butt and scarf joints as in Figs. 5 and 6. Generally, the stress tri-axiality of a torsional joint is lower than that of butt or scarf joints under tensile loading, where the deformability of the adhesive layer increases with the decrease of the stress tri-axiality [10]. This may be one reason why the difference of the breaking displacement between the acrylic and epoxy adhesives under torsional loading was greater than those of the butt and scarf joints under tensile loading.

Figure 8 shows failure envelopes for the acrylic and epoxy adhesives in the normal stress-shear stress plane. The plots were arranged from the strengths of the butt and scarf joints under tensile and shear load conditions. The tensile strengths of the bulk adhesive specimens are also indicated. As shown in this figure, the normal strength of the butt joint bonded with the epoxy adhesive is greater than the shear strength of the butt joint with thin-wall tube and the normal strength of the bulk specimen. Generally, an increase in the stress tri-axiality elevates the strength and reduces the toughness of materials [12]. This may be due to the stress tri-axiality of the butt joint under tensile loading being greater than that of the butt joint under torsional loading and that of the bulk adhesive specimen under tensile loading. However, for the acrylic adhesive, the normal strength of the butt joint is nearly equal to the shear strength of the butt joint with thin-wall tube and the normal strength of the bulk specimen. This indicates that for the acyclic adhesive the effect of the stress tri-axiality on the strength is small compared to that of the epoxy

adhesive. This figure also indicates that the strengths of the scarf joints are located on the lines between the butt joint and butt joint with thin-wall tube for both adhesives. The effect of stress triaxility on the fracture stress will be discussed in detail in the next clause.

Figure 9(a) and (b) show SEM images of fracture surfaces of the butt joint with the acrylic and epoxy adhesives under tensile loading. These figures show that the unevenness of the fracture surface for the butt joint with the acrylic adhesive is greater than that with the epoxy adhesive. SEM images of fracture surfaces under shear loading are shown in Figs. 9(c) and 9(d). For the acrylic adhesive, small blocks and deformed slender sticks are observed as in Fig.9(c). In contrast to the acrylic adhesive, a flat surface is observed for the epoxy adhesive as in Fig. 9(d). Hence, the SEM images in Fig. 7 indicate that the deformation of the fracture surface with acrylic adhesive is greater than that with the epoxy adhesive irrespective of the loading pattern.

3.2 Stress tri-axiality in the adhesive layer

Stress tri-axiality affects the strength of most polymeric materials [12]. The adhesive layer was usually restricted by a rigid bodies, wherein stress tri-axiality in the adhesive layer varies wide range depending on the kinds of the joints and loading conditions. Hence, estimating strength of the adhesively bonded joints, the stress tri-axiality in the adhesive layer should be taken into account.

In this study, stress tri-axiality parameter, σ_m/σ_{mie} were calculated for the adhesively bonded joints used in this experiment and bulk dumbbell specimen, where σ_m and σ_{mie} are mean and Miese equivalent stresses, respectively.

The stress tri-axiality parameters for the butt, scarf joints under tensile loading

were calculated under the following assumptions [13]: the adherends were treated as rigid bodes, and the stress distributions in the adhesive layer assumed to be uniform, which means that is stress singularity at the end of the adhesive/adherend interface was ignored.

Under the assumption as above mentioned, wherein coordinate system of the joints are set up as in Fig.10, normal and shear stresses to the adhesive layer, σ_y and τ_{xy} for the butt and scarf joints are given the following equations:

$$\sigma_y = \sigma_a sin^2\theta \qquad (2)$$

$$\tau_{xy} = \sigma_a sin\theta cos\theta \qquad (3)$$

As plane strain condition is assumed, σ_x and σ_z are given as follows:

$$\sigma_x = \sigma_z = \frac{v}{1-v}\sigma_a sin^2\theta \qquad (4)$$

The maximum and minimum principal stresses are given by

$$\sigma_1 = \frac{1}{2}\left\{\sigma_x + \sigma_y + \sqrt{(\sigma_x - \sigma_y)^2 + 4{\tau_{xy}}^2}\right\} \qquad (5)$$

$$\sigma_2 = \frac{1}{2}\left\{\sigma_x + \sigma_y - \sqrt{(\sigma_x - \sigma_y)^2 + 4{\tau_{xy}}^2}\right\}. \qquad (6)$$

For the scarf joint, the medium principal stress, is equal to the x or z directional stress, that is $\sigma_3 = \sigma_x = \sigma_z$.

Mises equivalent stress and mean stress are given by

$$\sigma_{mie} = \frac{1}{\sqrt{2}}\sqrt{(\sigma_1 - \sigma_2)^2 + (\sigma_2 - \sigma_3)^2 + (\sigma_3 - \sigma_1)^2)} \qquad (7)$$

$$\sigma_m = \frac{1}{3}(\sigma_1 + \sigma_2 + \sigma_3). \qquad (8)$$

Stress tri-axiality parameter, σ_m/σ_{mie} can be obtained from equations (7) and (8).

For the butt joint with thin wall tube under torsional loading, stress state in the adhesive layer can be treated as nearly pure shear stress condition, though a little

stress gradient appears in the adhesive layer due to the difference of outer and inner diameters of the specimen. Hence, following equations are obtained between the maximum, medium and minimum principal stresses:

$$\sigma_1 = -\sigma_3,\ \sigma_2 = 0 \qquad (9).$$

Shear stress, τ_0 in the adhesive layer is given by

$$\tau_0 = \sigma_1 \qquad (10).$$

From equations (9) and (10), Mises equivalent stress and mean stress are given by

$$\sigma_{mie} = \frac{1}{\sqrt{2}}\sqrt{(\sigma_1 - \sigma_2)^2 + (\sigma_2 - \sigma_3)^2 + (\sigma_3 - \sigma_1)^2} = \sqrt{3}\sigma_1 = \sqrt{3}\tau_0 \quad (11)$$

$$\sigma_m = \frac{1}{3}(\sigma_1 + \sigma_2 + \sigma_3) \qquad (12).$$

Hence, stress tri-axiality parameter, σ_m/σ_{mie} is zero under torsional loading.

For the bulk dumbbell specimen under tensile loading, Mises equivalent stress and mean stress are given by

$$\sigma_{mie} = \sigma_a \qquad (13)$$

$$\sigma_m = \frac{1}{3}(\sigma_1 + \sigma_2 + \sigma_3) = \frac{1}{3}\sigma_a \qquad (14).$$

Where σ_a is tensile stress. From equations (13) and (14), stress tri-axiality parameter, σ_m/σ_{mie} is 1/3 for the dumbbell specimen under tensile loading.

Figure 11 shows the effect of stress triaxility on the fracture stress for the adhesively bonded joints and dumbbell specimen, wherein the fracture stresses are arranged by the maximum principal stress in the adhesive layer: the maximum principal stresses for the butt and scarf joints are calculated form equation (7), one for the butt joint with thin wall tube agrees with the shear stress in the adhesive layer as indicated by equation (10). As shown in Fig.11, the maximum principal stress for the epoxy adhesive increases with the stress triaxility parameter, whereas that for

the acrylic adhesive dose not vary with the stress triaxility parameter. For many polymeric materials, It is observed that an increase in the stress triaxility parameter leads to alternating the fracture mode from ductile to brittle, and also makes the strength increased [12]. This trend agrees with that of the epoxy adhesive. On the other hand, the fracture mode for the acrylic adhesive was ductile independent on kinds of the joints. This may be one reason why the fracture stress dose not vary with the stress triaxility parameter.

3.3 Fracture toughness of the adhesively-bonded DCB specimens

Figure 12 shows example load displacement curves for the adhesively bonded DCB specimens with the epoxy and acrylic adhesives. As shown in this figure, for the epoxy adhesive the load rapidly drops from the peak load, whereas the slope from the peak load is gentle for the acrylic adhesive. This means that the crack propagated rapidly for the epoxy adhesive and gradually for the acrylic adhesive. Figure 13 shows microscope images near the crack tip in the adhesive layer for the DCB joint with the acrylic adhesive, that is, this figure indicates the damage evolution process near the crack tip. Just before the peak point as in Fig. 13(a), a stress whitening zone appears in front of the pre-crack. Then, at the peak point as in Fig. 13(b), the stress whitening intensifies and blunting of the crack tip proceeds. Just after the peak point, further stress whitening proceeds and small voids appear in the stress whitening zone as in Fig. 13(c). When the applied load decreases further, crack growth is observed as in Fig. 13(d).

Figure 14 shows the relationship between the critical energy release rate and crack growth. In Fig. 14, for the acrylic adhesive, G_{IC} increases continuously with crack growth. This means that R-curve behavior is observed for the acrylic adhesive.

For the epoxy adhesive, stick-slip crack propagation behavior was observed as in Fig. 12, hence G_{IC} varies discretely with crack length, and G_{IC} is independent of the crack growth and distributes around form 1000 J/m^2 to 2000 J/m^2. The maximum value of G_{IC} for the acrylic adhesive was a little higher than upper value of G_{IC} for the epoxy adhesive.

Figure 15(a) and (b) show macroscopic views of the fracture surfaces of the DCB specimens with the acrylic and epoxy adhesives, respectively. As shown in Fig. 15(a) and (b), cohesive fracture is observed for the both adhesives. Further observation indicates that the fracture surface is relatively flat for the acrylic adhesive, whereas for the epoxy adhesive the fracture surface is more smooth and curved arrest lines are observed. Figure 16(a) and (b) show SEM images of fracture surfaces for the DCB joints with the acrylic and epoxy adhesives, respectively. Although some grooves are observed on the surface with the acrylic adhesive and small steps are observed on the surface with the epoxy adhesive, these deformations of the surfaces with both adhesives are small compared to those of butt joints under tensile and torsional loadings as in Fig. 9(a) and (b). This may be due to the stress tri-axiality in the adhesive layer for the DCB joints being higher than those for the butt joints.

3.4 Tensile shear strength of the adhesively bonded lap joints

Figure 17 shows load-displacement and crack length-displacement curves for the lap joints with the epoxy and acrylic adhesives whose the lap length was 50 mm. As mentioned above, to measure the crack growth, crack gauges were pasted on the lap end where the cracks initiate. In this figure, P_i is defined the load, when the crack growth initiates. As shown in this figure, the cracks initiate at the point where

the load-displacement curve deviates from the linearity for the both adhesives. Further observation indicates that the crack propagation period for the epoxy adhesive is much smaller than that for the acrylic adhesive.

Figure 18 shows the relationship between P_i/P_{max} and lap length for the epoxy and the acrylic adhesives. In this figure, P_i and P_{max} indicate the load for crack initiation and the maximum load, respectively. Hence, the small and large values of P/P_{max} mean that the crack initiated in the early stage of the fracture process and the crack propagates immediately just after the crack initiation, respectively. In Fig. 18, for the epoxy adhesive the crack initiates at about 98% of the fracture load irrespective of the lap length, whereas for the acrylic adhesive P/P_{max} decreases with the increase of the lap length. This indicates that the fracture for the epoxy adhesive occurs immediately after crack initiation, whereas for the acrylic adhesive the crack propagation period increases with increasing lap length.

Figure 19 shows the relationship between shear strength and lap length for the epoxy and the acrylic adhesives. As shown in this figure, shear strength decreases with increasing lap length for both adhesives. More detailed observation indicates that shear strength with the epoxy adhesive rapidly decreases with increasing lap length, whereas the shear strength with the acrylic adhesive decreases gently with increasing lap length. When the lap length is 10 mm, the shear strength of the joint with the epoxy adhesive is about 2 times as high as that with acrylic adhesive. However, when the lap length is 70 mm, the shear strength of the joint with the epoxy adhesive is only about 1.3 times higher than that with acrylic adhesive. Incidentally, the ductility of the acrylic adhesive is higher than that of the

epoxy adhesive. For the lap joints, lap end is stress singularity point where the crack initiates. Generally, sensitivity for stress singularity are high for the brittle material and low for the ductile material. For the lap joints, intensity of stress singularity increases with the lap length. Therefore, it is assumed that the strength for the brittle material is sensitive with increasing the lap length, whereas strength for the brittle material is blunt to the increase of the lap length. Furthermore, stable crack propagation was observed for the acrylic adhesive, whereas the crack propagates rapidly for the epoxy adhesive as in Fig. 17. We considered that the crack propagation period increases with lap length for acrylic adhesive. As above two points i.e. sensitivity for the stress singularity and crack propagation period may be also reasons why the decrease of the shear strength due to the increase of the lap length with the acrylic adhesive is more gentle than that of the epoxy adhesive.

Figure 20 (a) and (b) show SEM images of the fracture surfaces for the lap joints with the acrylic and epoxy adhesives, respectively. For the acrylic adhesive, several craters with relative large diameter are observed as in Fig. 20(a). In Fig. 20(b), although a conspicuous groove is observed in the fracture surface with the epoxy adhesive, the majority of the fracture surface is relatively flat and the deformation of the fracture surface with acrylic adhesive is greater than that with the epoxy adhesive. These observations are similar to the SEM observations for the other types of joints.

4. Conclusions

The fracture characteristics of epoxy and acrylic adhesives were compared using several kinds of adhesively bonded joint. The main results obtained in this

work were as follows:

(1) The results of tensile tests for the butt and scarf joints and torsional tests for the butt joint with thin-wall tube were arranged in the normal stress-shear stresses plane. The strengths of the joints made with the epoxy adhesive were over 4 times greater than those made with the acrylic adhesive, irrespective of joint type. The normal strength of the butt joint bonded with the epoxy adhesive was greater than the shear strength of the butt joint with thin-wall tube and the normal strength of the bulk specimen, whereas the normal strength of the butt joint with the acrylic adhesive was nearly equal to the shear strength of the butt joint with thin-wall tube and the normal strength of the bulk specimen.

(2) Strengths for the butt and scarf joints under tensile loading and those for the butt joint with thin-wall tube under torsional loading were arranged by the maximum principal stress, and the effect of stress triaxility parameter on the maximum principal stress was investigated. As a result, the maximum principal stress for the epoxy adhesive increases with stress tri-axiality parameter, σ_m/σ_{mie}, whereas that for the acrylic adhesive dose not vary with the stress triaxility parameter.

(3) Stick-slip type crack propagation was observed for the DCB joint with the epoxy adhesive, whereas stable crack propagation was observed for that with the acrylic adhesive. From the relationship between G_{IC} and crack length for both adhesives, R-curve behavior was observed for the acrylic adhesive, whereas for the epoxy adhesive, G_{IC} varies discretely with crack length, and G_{IC} was independent of the crack growth.

(4) Load-displacement curves for the lap joints with both adhesives indicated that cracks initiated at the point where the load-displacement curve deviated from

linearity, and that the crack propagation period for the epoxy adhesive was much smaller than that for the acrylic adhesive. Comparing the relationship between shear strength and lap length, the shear strength of the lap joint with the epoxy adhesive rapidly decreased with increasing lap length, whereas that with the acrylic adhesive decreased gently with increasing the lap length. Hence, the difference between the shear strength with the epoxy adhesive and that with the acrylic adhesive decreased with the lap length.

References

[1] Charnock RS, Structural acrylic adhesives for the sheet steel fabrication industries. Int J Adhesion Adhesives 1985:5:201-206.

[2] Pereira AB, de Morais AB, Strength of adhesively bonded stainless steel joints. Int J Adhesion Adhesives 2003:23:315-322.

[3] Gallio G, Lombardi M, Rovarino D, Fino P, Montanaro, Influence of the mechanical behavior of different adhesives on an interference-fit cylindrical joint. Int J Adhesion Adhesives 2013:47:63-68.

[4] Boyd SW, Winkle IE, Day AH, Bonded butt joints in pultruded GRP panels-an experimental study. Int J Adhesion Adhesives 2004:24:263-275.

[5] De Castro J, Keller T, Ductile double-lap joints form brittle GFRP laminates and ductile adhesives, Part 1:Experimental investigation. Composites Part B 2008;39:271-281.

[6] Yadollahi M, Barkhordari S, Gholamali I, Farhoudian S, Effect of nanofillers on adhesion strength of steel joints bonded with acrylic adhesive. Sci. Tech. of Welding and Joining 2015:20:443-450.

[7] Barton L, Birkett M, Mechanical behavior of adhesively bonded polyethylene tapping tees. Int J Adhesion Adhesives 2016:66:1-8.

[8] Park S, Dillard DA, Development of a simple mixed-mode fracture test and the resulting fracture energy envelope for an adhesive bond. Int. Jour. Fract. 2007:148:261-271.

[9] Hand HM, Arah CO, McNamara DK, Mecklenburg MF, Effects of environmental exposure an adhesively bonded joints. Int J Adhesion Adhesives 1991:11:15-23.

[10] Imanaka M, Fujimani A, Suzuki Y, Fracture and Yield behavior of adhesively bonded joints under triaxial stress conditions, J Mater Sci 2000:35:2481-2491.

[11] Imanaka M, Motohashi S, Nishi K, Nakamura Y, Kimoto M, Crack-growth behavior of epoxy adhesives modified with liquid rubber and cross-linked rubber particles under mode Ⅰ loading, Int. Jour. of Adhesion Adhesives 2009:29:45-55.

[12] Ward IM, Hadley DW, An introduction to the mechanical properties of solid polymers. John Wiley & Sons Ltd, 1993:214-244.

[13] Suzuki Y, Three-dimensional finite element analysis of adhesive scarf joints of steel plates loaded in tension. Bulletin of JSME 1984:27:1836-1846.

Table 1 Mechanical properties of epoxy and acrylic adhesives.

Adhesives	**Curing temperature（℃）**	**Curing time（h）**	**Young's modulus（MPa）**	**Poisson's ratio**	**Glassy-transition temperature (℃)**
Epoxy adhesive（SUNRISE MSI Co. :E56）	180	1	3377	0.37	110
Acrylic adhesive（DENKI KAGAKU KOGYO Co. C-355-20）	Room temperature	24	294	0.44	94

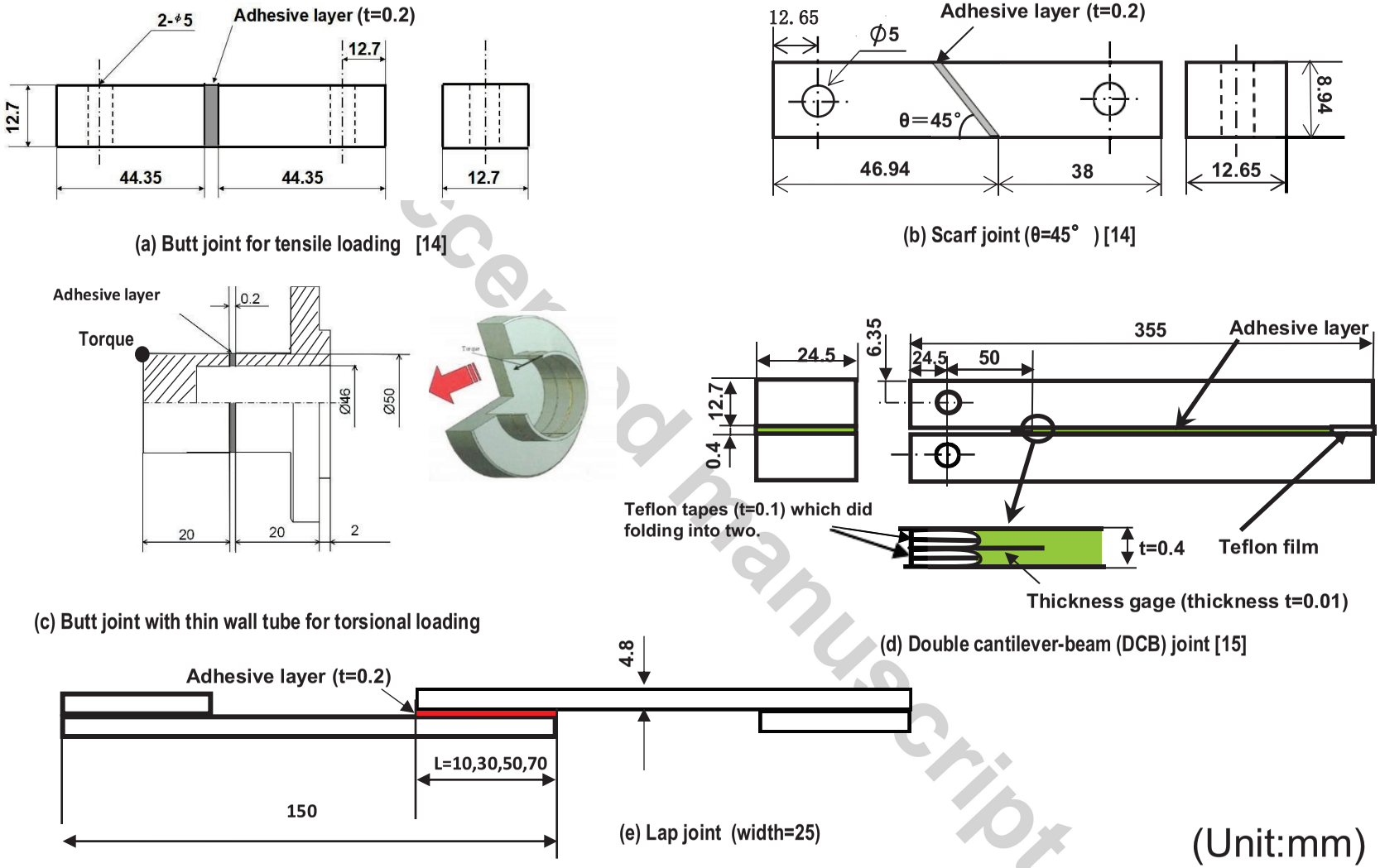

Fig. 1 Shape and dimensions of the adhesively bonded butt, scarf, lap and DCB joints (dimensions in mm).

(a) Butt joint under tensile loading

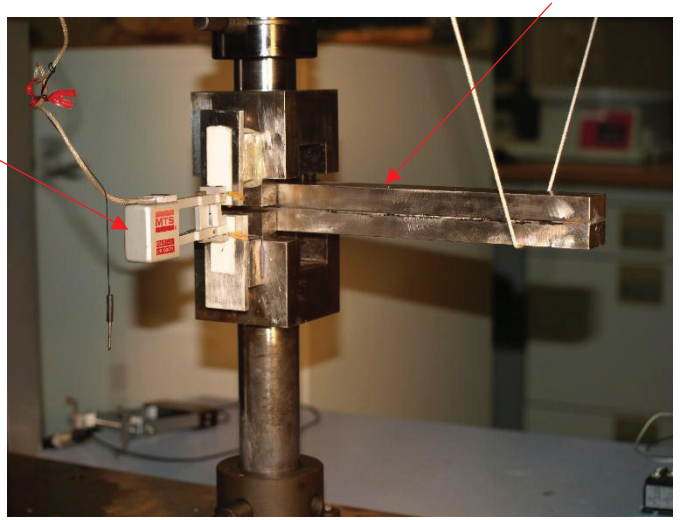

(b) DCB specimen under tensile loading

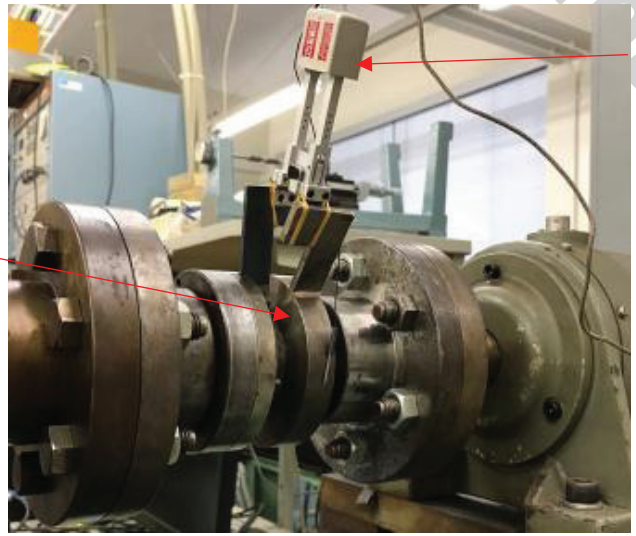

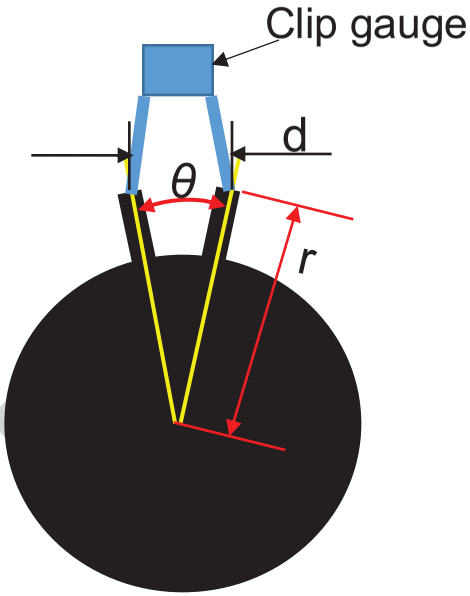

(c) Butt joint with thin wall tube under torsional loading.

Fig. 2 Experimental setup for adhesively bonded specimens.

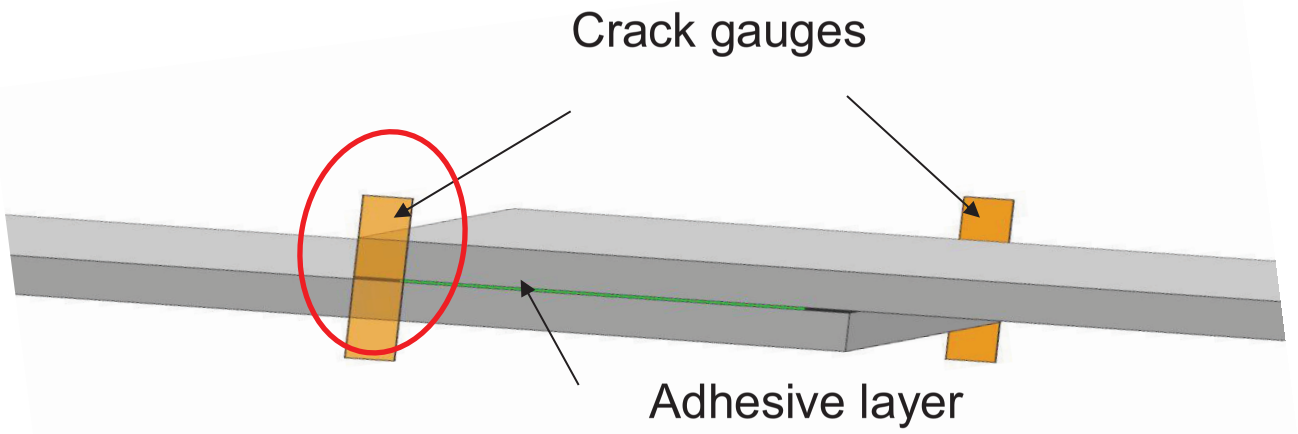

(a) The locations of crack gauges on a lap joint.

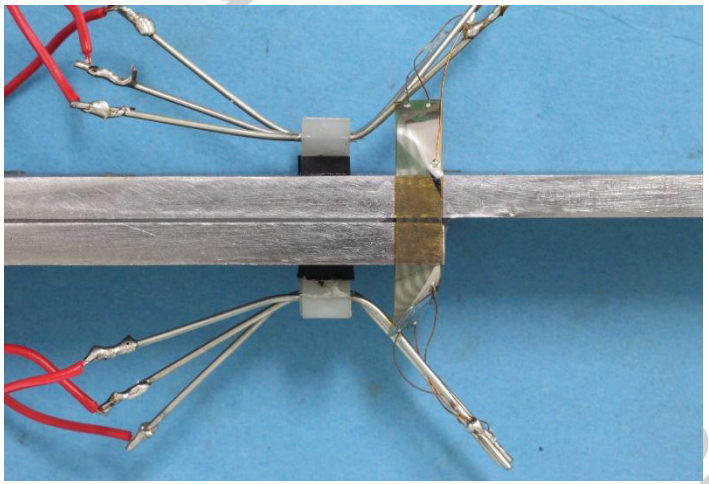

(b) Photo of a crack gauge bonded onto the adhesive layer.

Fig.3 Illustration for measurement of crack growth from lap ends using crack gauges.

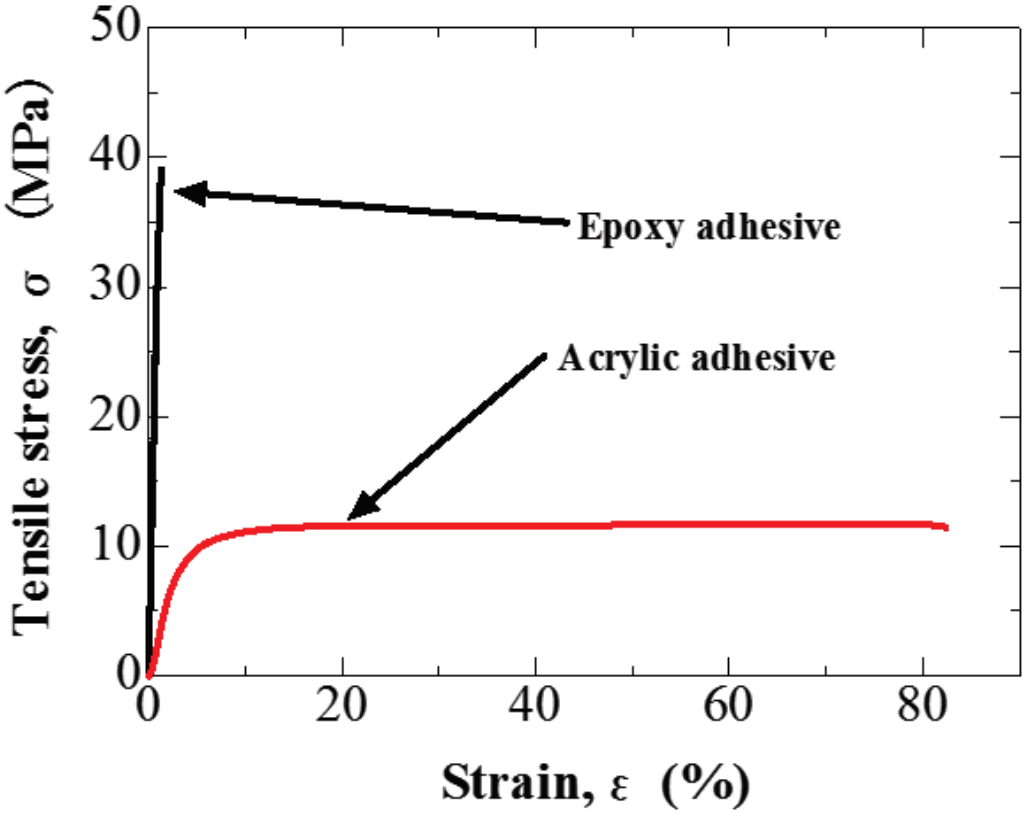

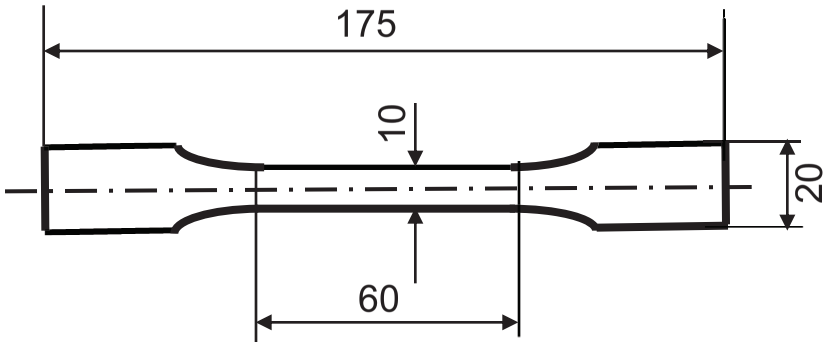

Shape and sizes of bulk specimen used for tensile test (t=2mm).

Fig. 4 Stress-strain curves for the bulk adhesives.

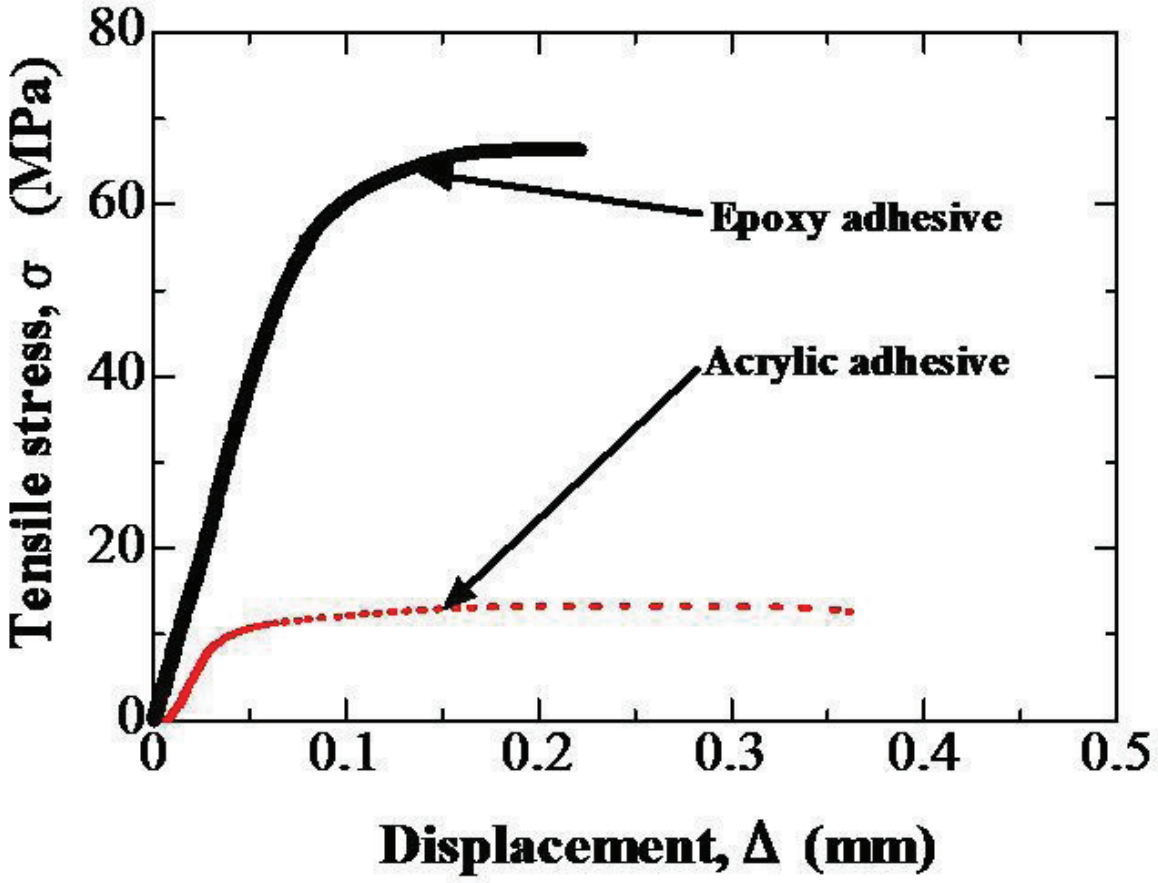

Fig. 5 Stress-displacement curves for the butt joints under tensile loading.

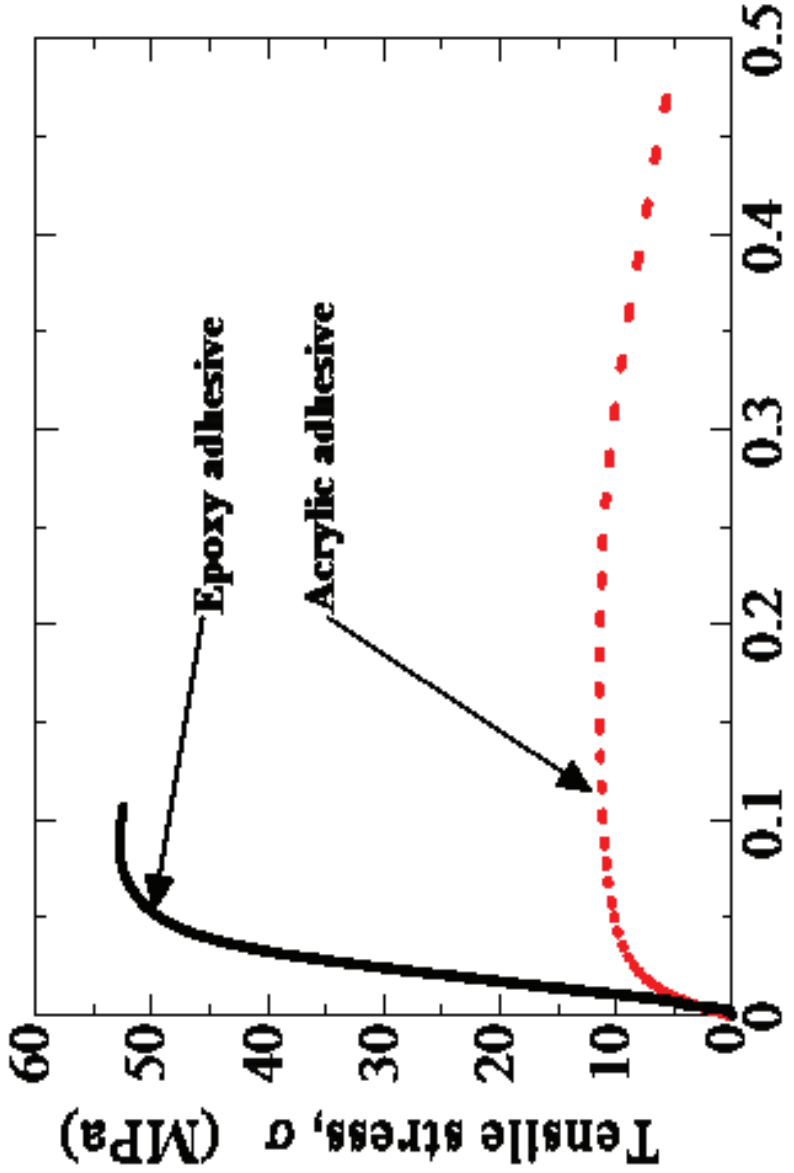

Fig. 6 Stress-displacement curves for the scarf joint under tensile loading (θ=45°).

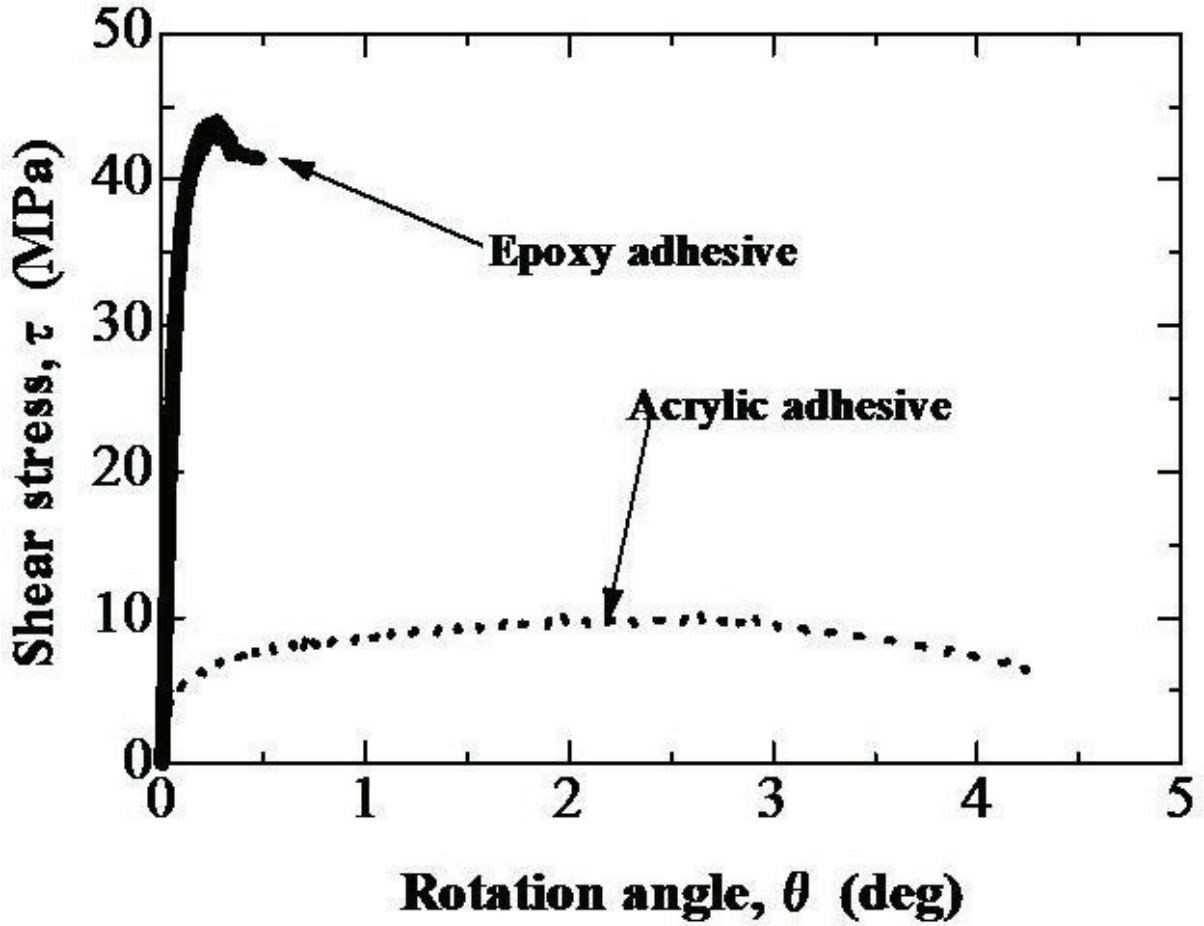

Fig. 7 Stress-rotation angle curves for the butt joints with thin-wall tube under torsional loading.

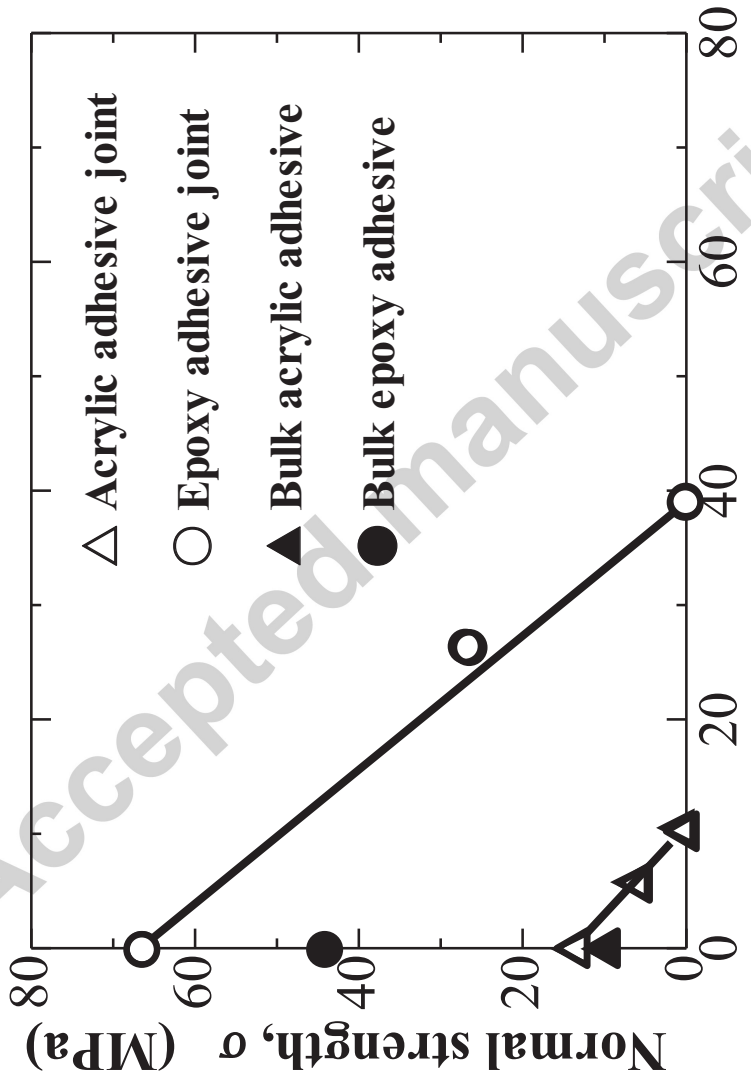

Fig. 8 Failure envelopes in the normal stress-shear stress plane.

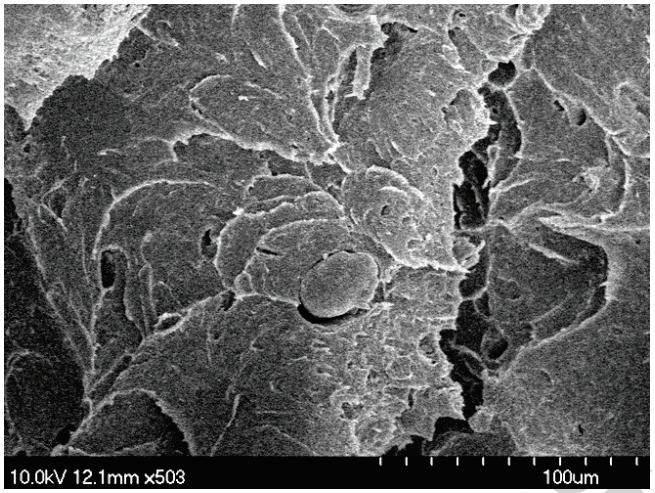

Loading direction

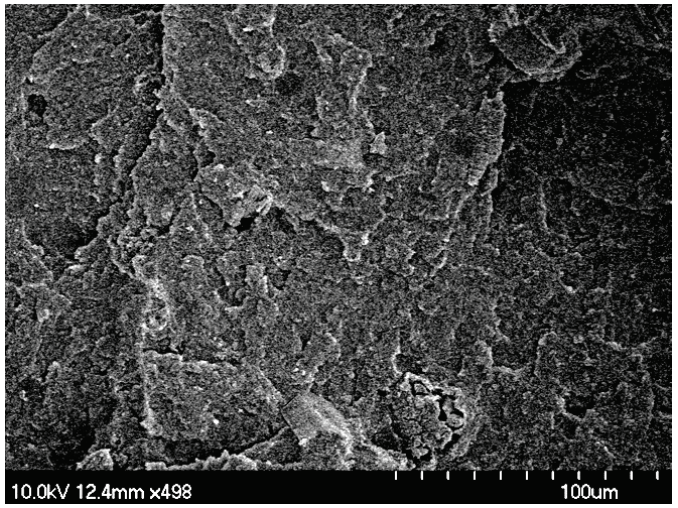

(a) Acrylic adhesive under tensile loading

(b) Epoxy adhesive under tensile loading

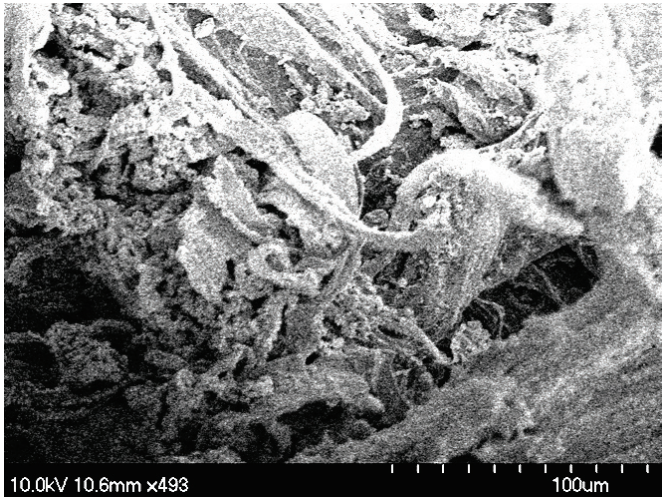

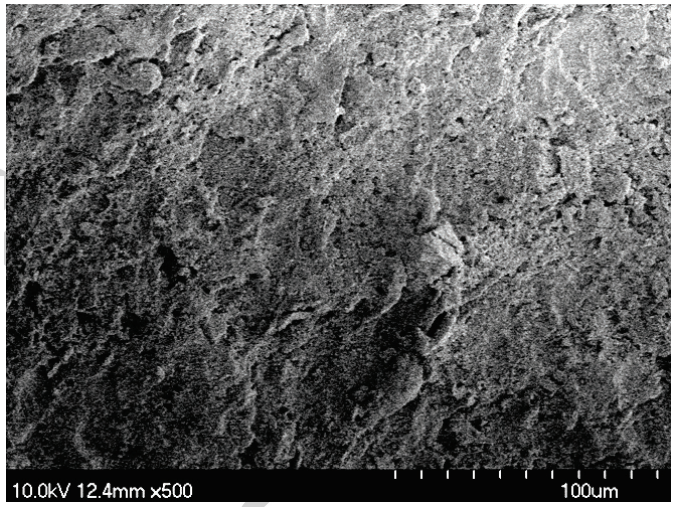

(c) Acrylic adhesive under shear loading

(d) Epoxy adhesive under shear loading

Fig.9 SEM images of fracture surfaces of the butt joint under tensile loading and the butt joint with thin-wall tube under torsional loading.

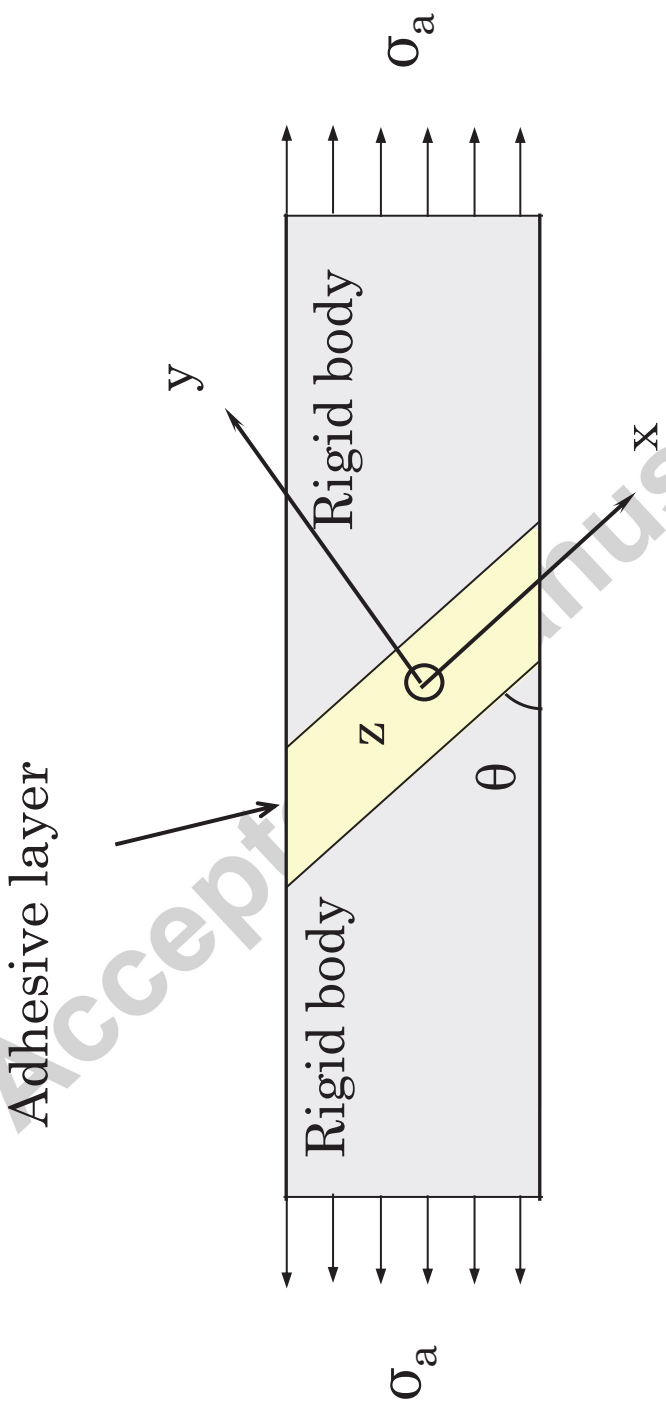

Fig.10 Coordinate system of scarf joint.

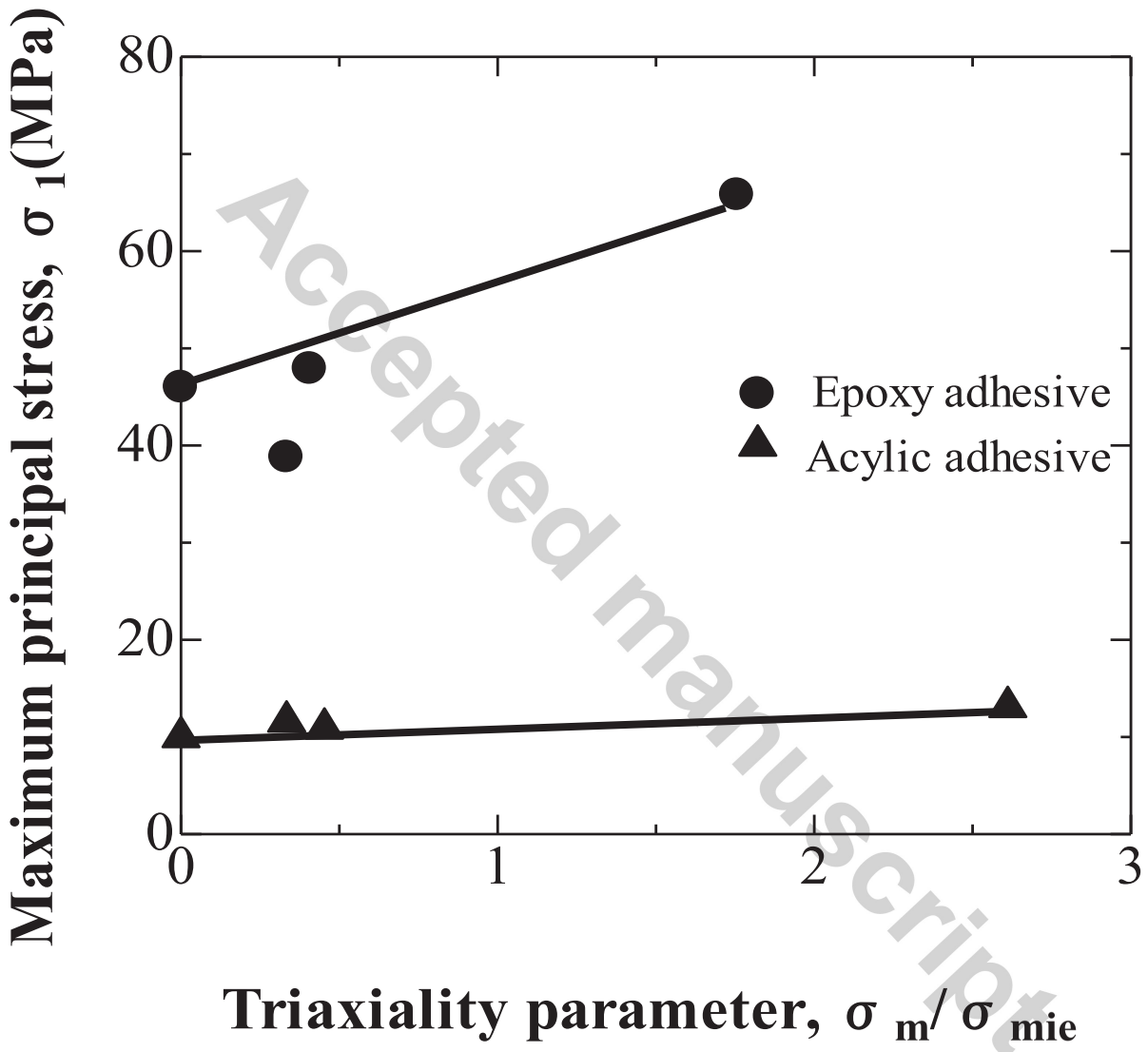

Fig.11 Effect of stress triaxiality parameter on the maximum principal stress in the adhesive layer.

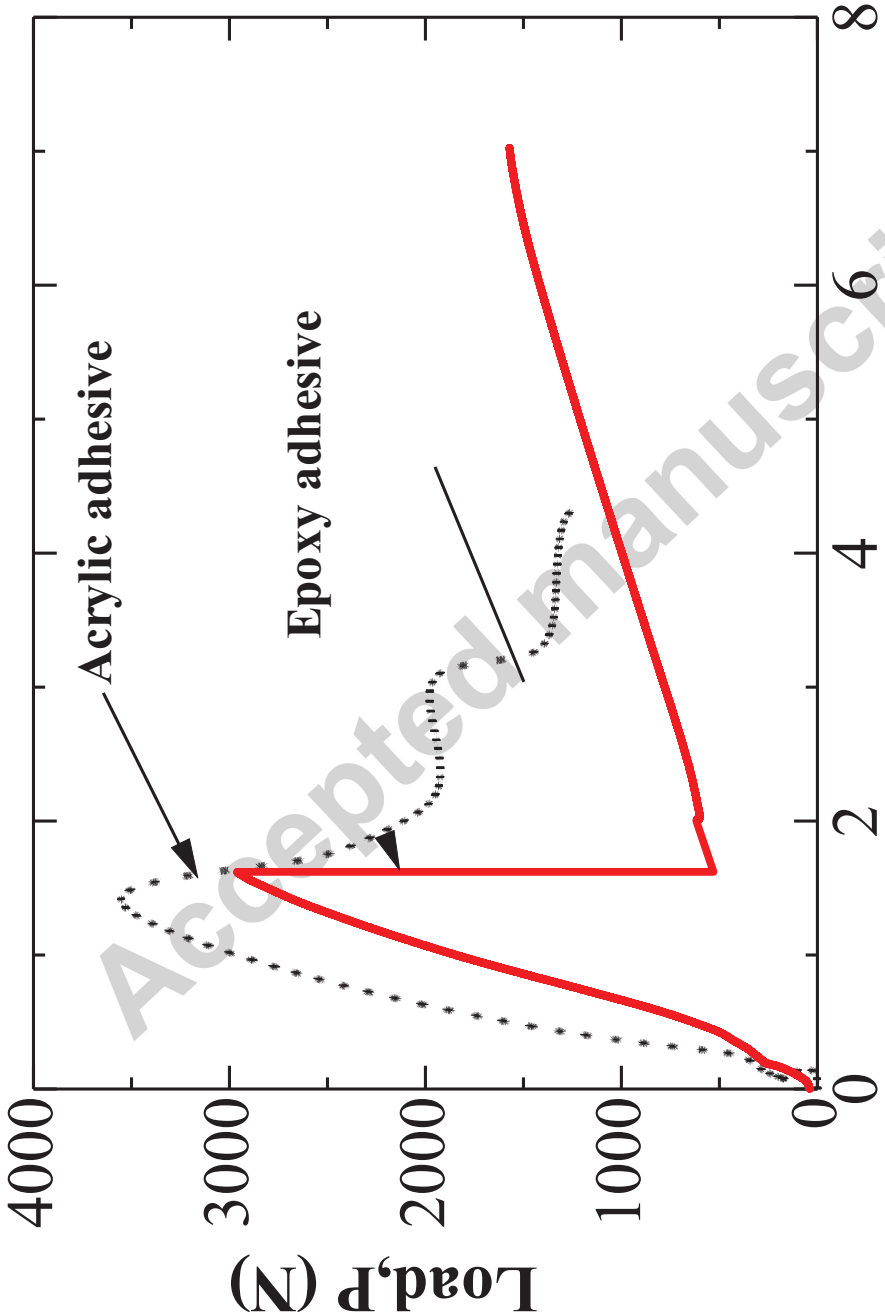

Fig. 12 Typical load-displacement curves for the DCB joints.

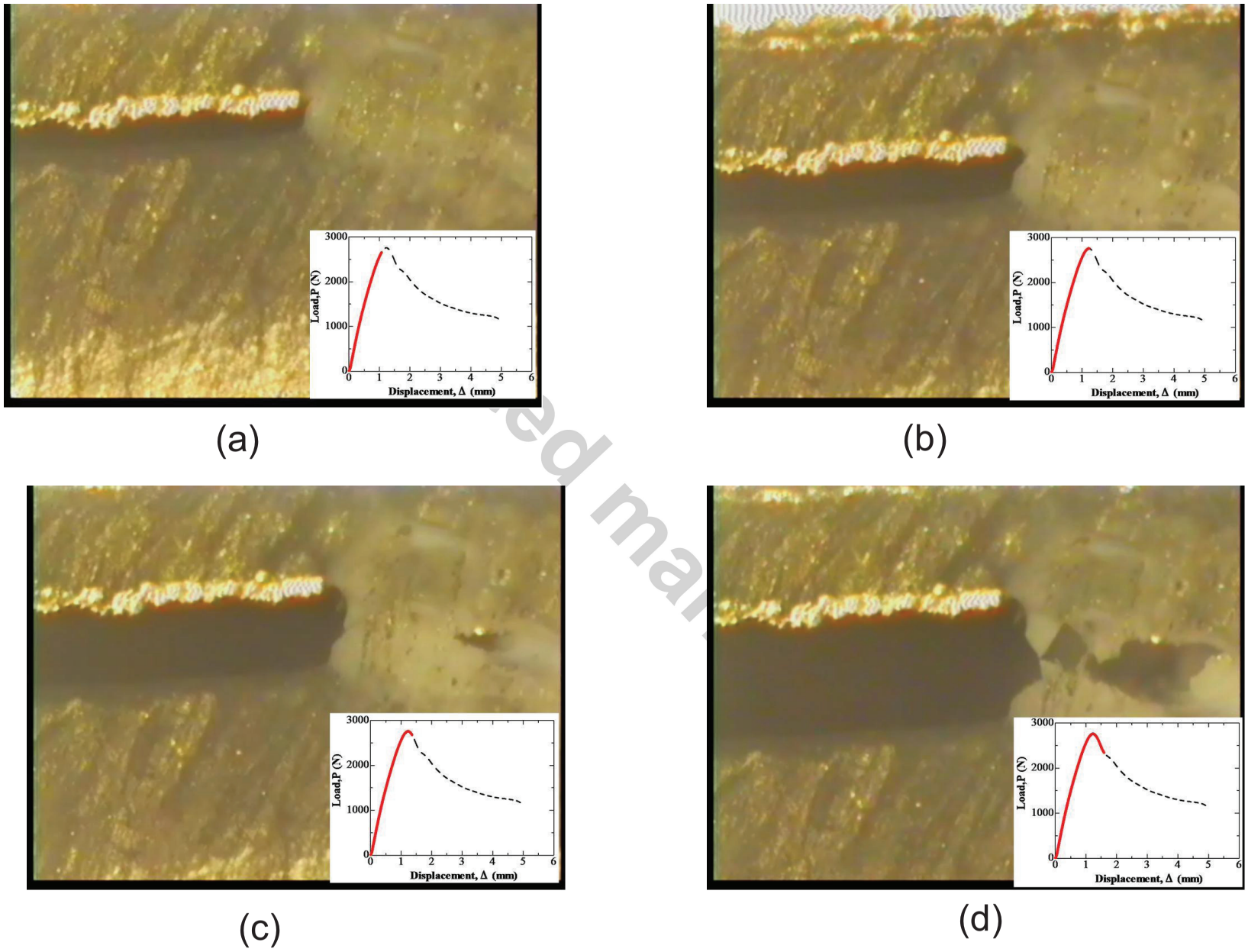

Fig. 13 The entire sequence of the failure process in the adhesive layer for the DCB joint with the acrylic adhesive.

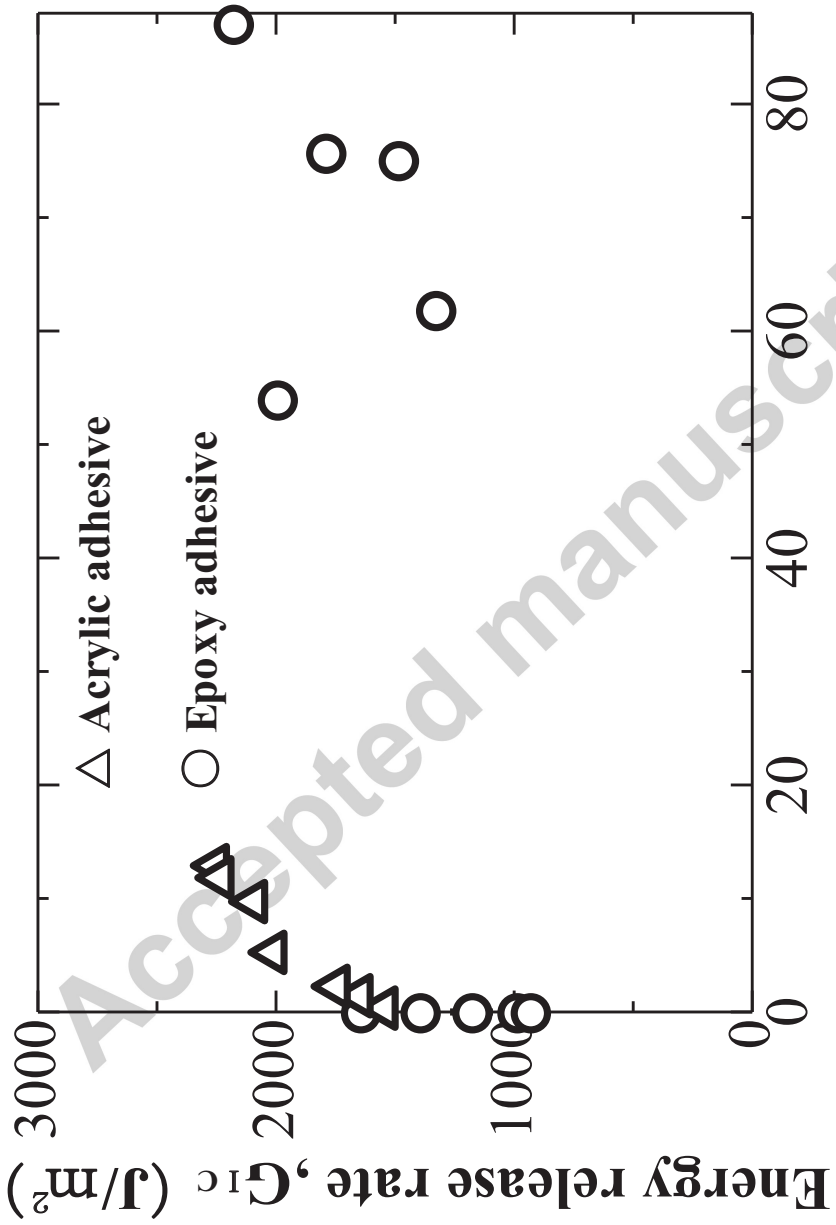

Fig. 14 Relationship between critical energy release rate and crack growth.

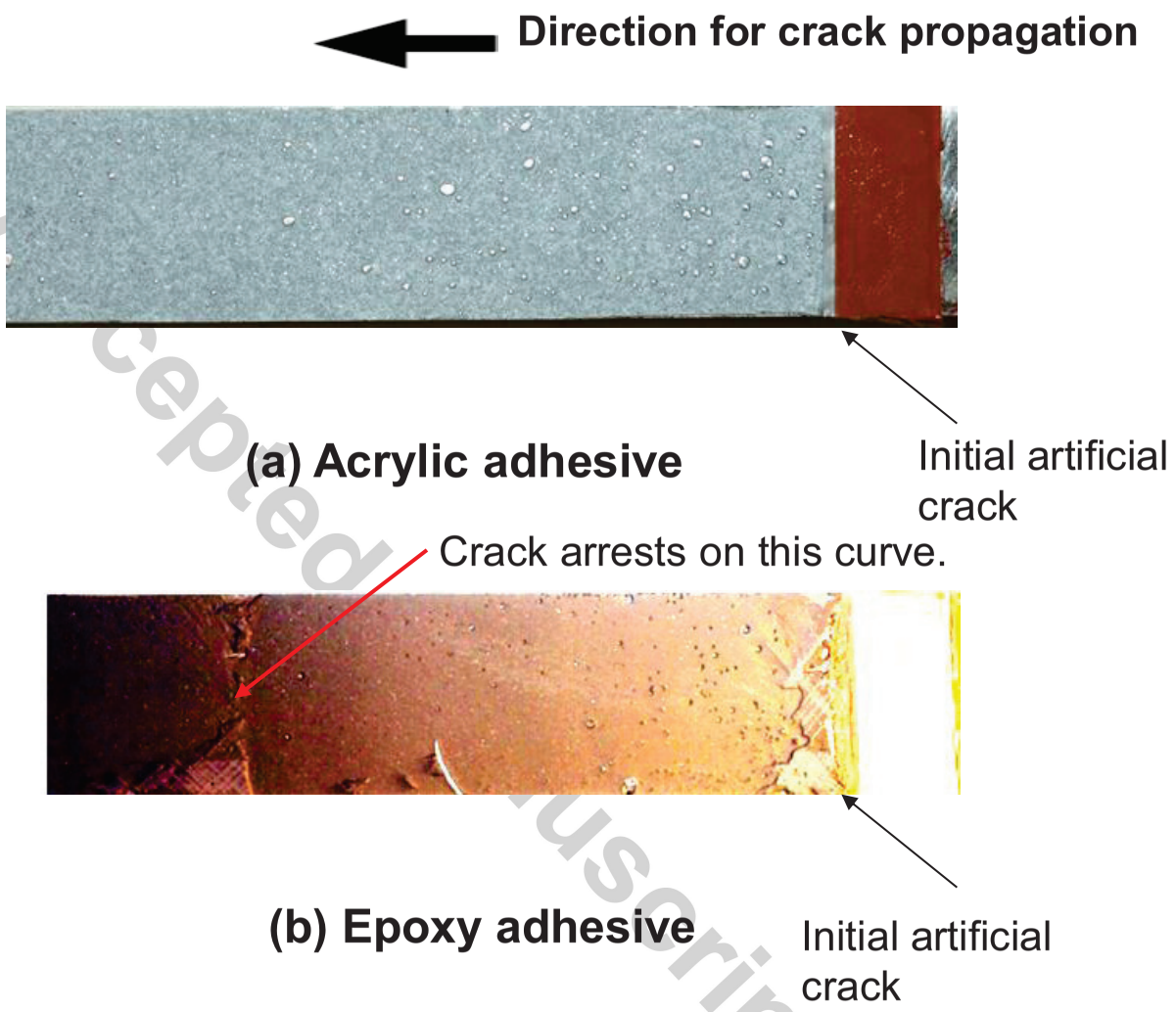

Fig.15 Fracture surfaces of the DCB joints.

Loading direction

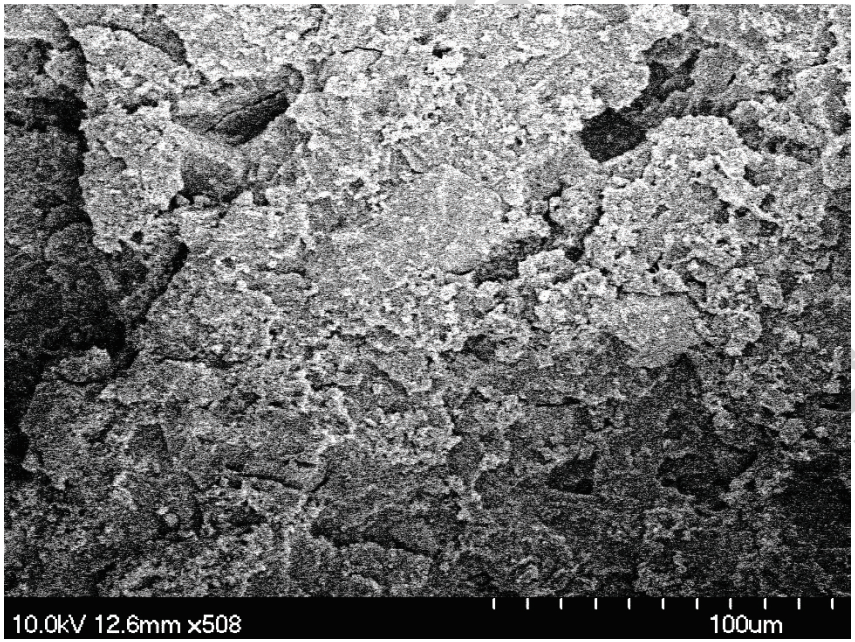

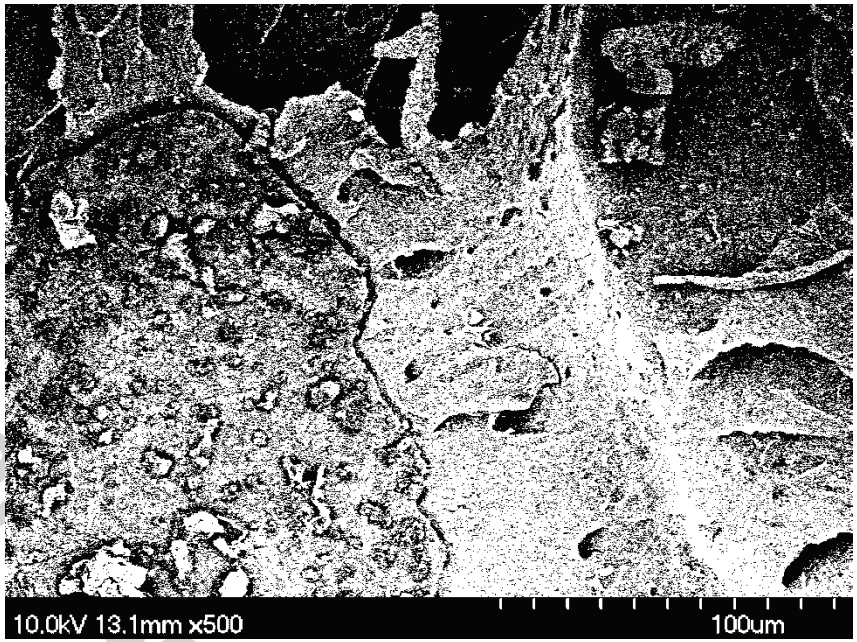

(a) Acrylic adhesive **(b) Epoxy adhesive**

Fig. 16 SEM images of the fracture surfaces for the DCB joints.

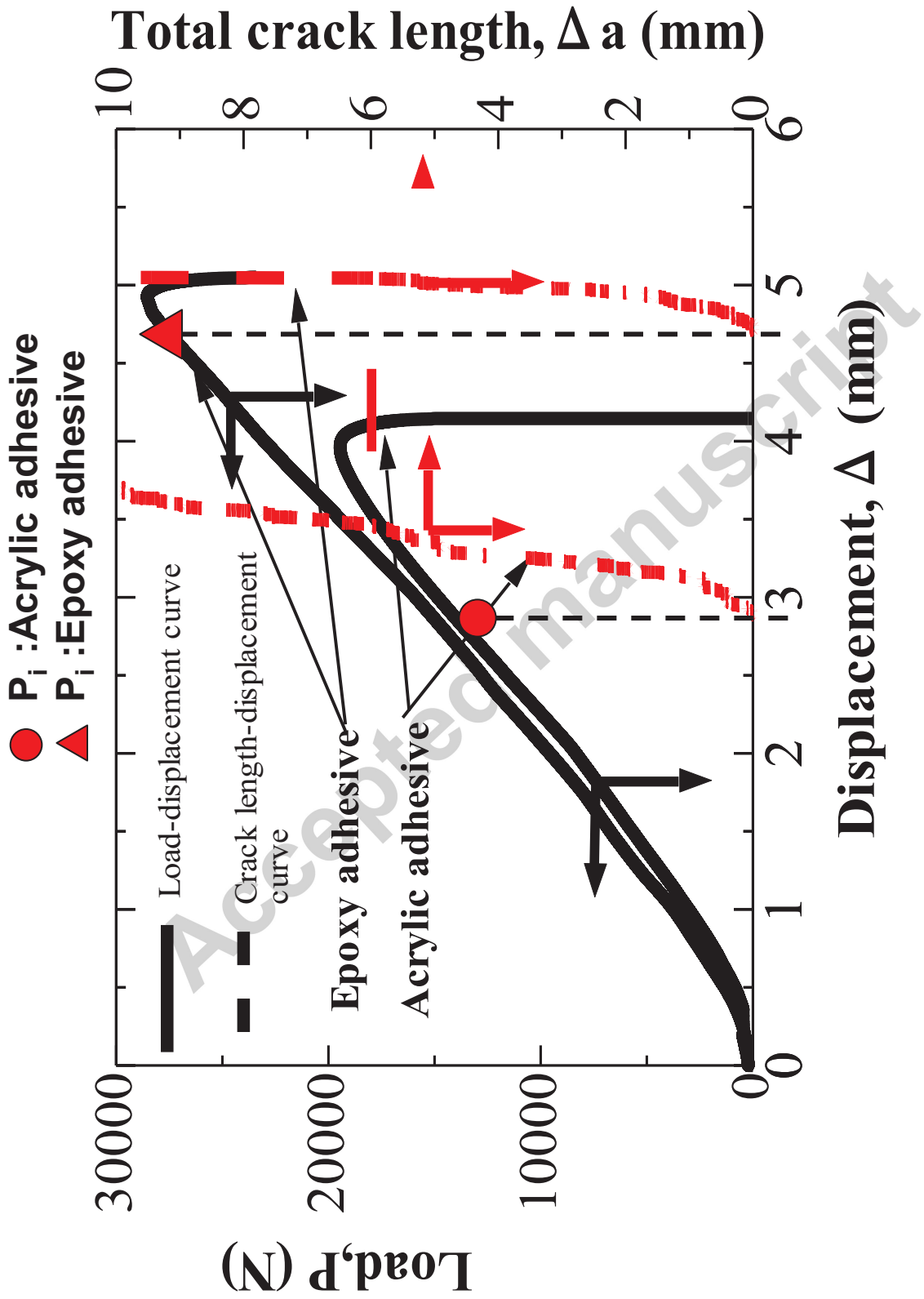

Fig. 17 Load and crack length versus displacement for the single lap joints (L=50 mm).

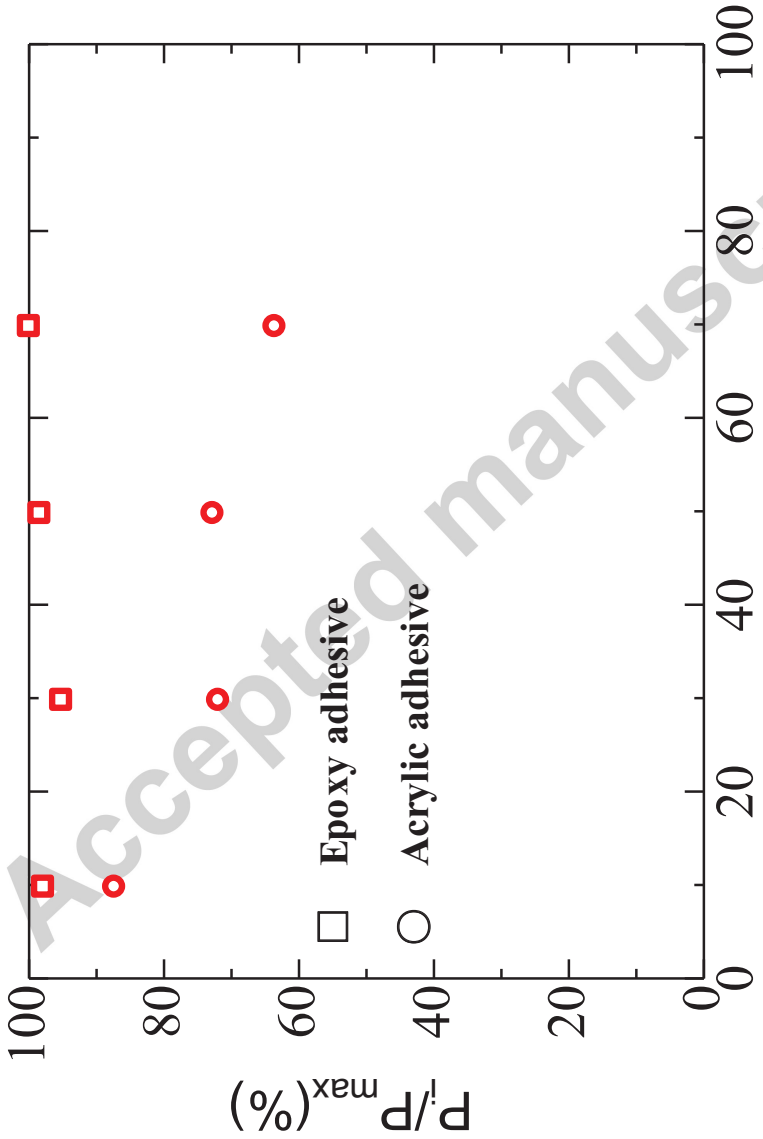

Fig. 18 P_i/P_{max} vs. lap length.

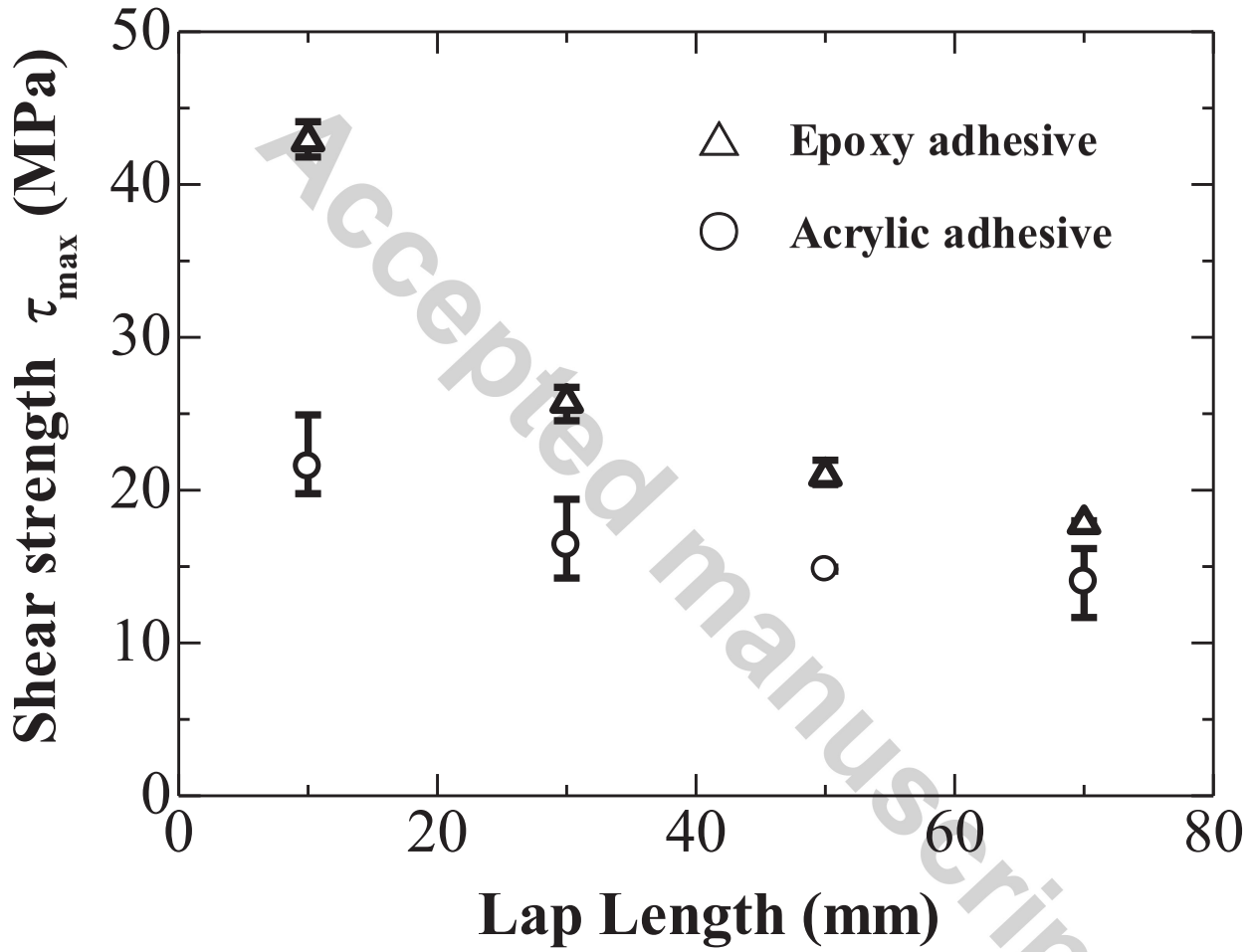

Fig. 19 Relationship between shear strength and lap length.

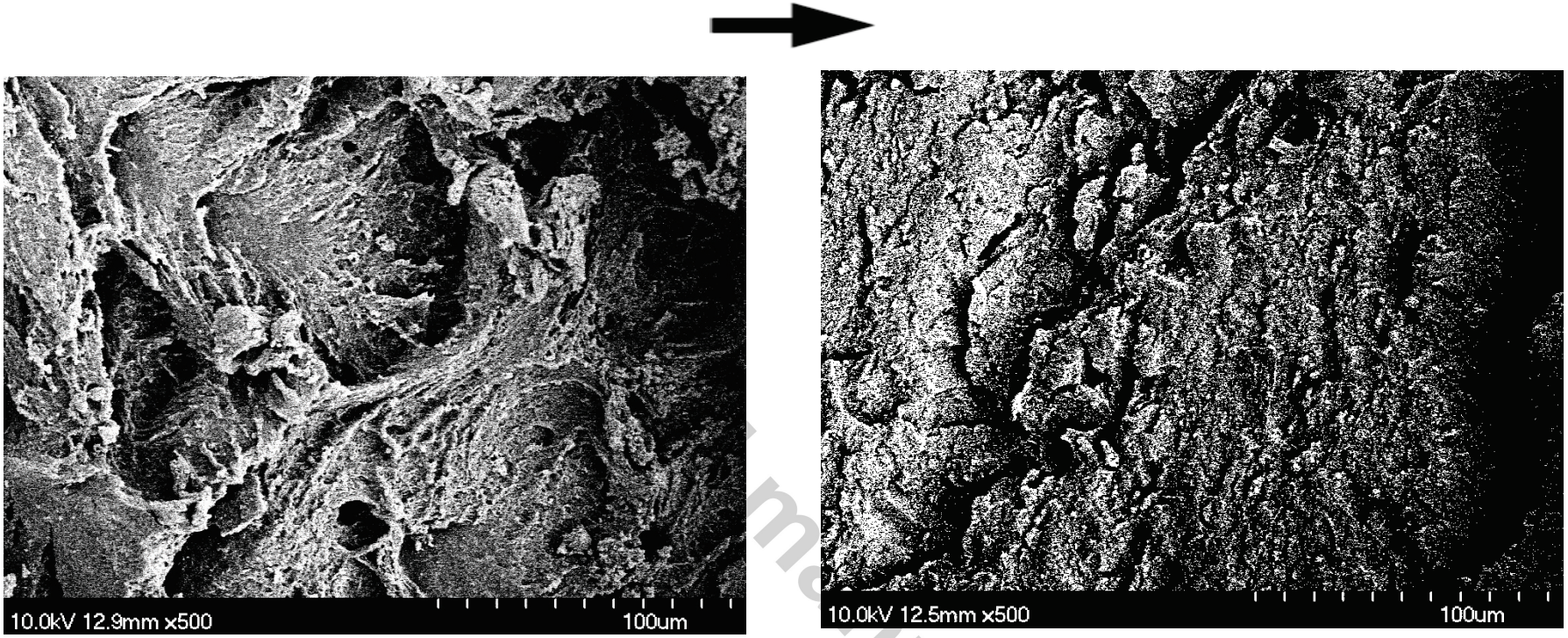

(a) Acrylic adhesive **(b) Epoxy adhesive**

Fig. 20 SEM images of the fracture surfaces for the lap joints (L=50 mm).